Carbohydrate Polymers 95 (2013) 207–213

Contents lists available at SciVerse ScienceDirect

Carbohydrate Polymers

journal homepage: www.elsevier.com/locate/carbpol

Plantain starch granules morphology, crystallinity, structure transition, and size evolution upon acid hydrolysis

C. Hernández-Jaimes[a], L.A. Bello-Pérez[b,1], E.J. Vernon-Carter[c,*], J. Alvarez-Ramirez[c]

[a] Universidad Autónoma Metropolitana-Iztapalapa, Departamento de Biotecnología, Apartado Postal 55-534, México, D.F. 09340, Mexico
[b] Centro de Desarrollo de Productos Bióticos (CEPROBI) del Instituto Politécnico Nacional, Yautepec, Morelos, Mexico
[c] Universidad Autónoma Metropolitana-Iztapalapa, Departamento de Ingeniería de Procesos e Hidráulica, Apartado Postal 55-534, México, D.F. 09340, Mexico

ARTICLE INFO

Article history:
Received 10 December 2012
Received in revised form 28 February 2013
Accepted 2 March 2013
Available online 13 March 2013

Keywords:
Plantain starch
Acid hydrolysis
Kinetics
Morphology
Crystallinity

ABSTRACT

Plantain native starch was hydrolysed with sulphuric acid for twenty days. Hydrolysis kinetics was described by a logistic function, with a zero-order rate during the first seven days, followed by a slower kinetics dynamics at longer times. X-ray diffraction results revealed a that gradual increase in crystallinity occurred during the first seven days, followed by a decrease to values similar to those found in the native starch. Differential scanning calorimetry analysis suggested a sharp structure transition by the seventh day probably due to a molecular rearrangement of the starch blocklets and inhomogeneous erosion of the amorphous regions and semi crystalline lamellae. Scanning electron micrographs showed that starch granules morphology was continually degraded from an initial oval-like shape to irregular shapes due to aggregation effects. Granule size distribution broadened as hydrolysis time proceeded probably due to fragmentation and agglomeration phenomena of the hydrolysed starch granules.

1. Introduction

Starch, a natural homo-polysaccharide of glucose monomers extracted from diverse botanical sources (tubers, cereals, legumes and unripe fruits), is an abundant, renewable, biodegradable and inexpensive material with a wide variety of applications in food and non-food industry (Bello-Pérez & Paredes-López, 2009). Starch is organized in small granules, where size and shape as well as physicochemical and functional properties are specific of botanic origin (Biliaderis, 1991). These features depend of the internal organization and relative composition of the main starch components given by amylose and amylopectin. Starch is considered as semi-crystalline polymer since amorphous and crystalline zones are combined within growth rings with complex geometric arrangements with nano-sized blockets (Oates, 1997). Crystalline lamellae in the blockets are organized as amylopectin double helices formed by intertwining chains of more than ten glucose units. Branching points are found in the amorphous lamellae (Gallant, Bouchet, & Baldwin, 1997). It is commonly accepted that blockets in B- and C-type starches are of the order of 400–500 nm, while in A-type starches of the order of 20–100 nm (Gallant et al., 1997).

Fabrication of nano- and micro-particles from biopolymers can be utilized as delivery systems or to modulate the physicochemical or sensory characteristics of food products. Such is the case of starch, which is rarely used in its native form. In fact, different chemical and physical methods have been designed in order to modify starch structural and functional properties. Digestibility, biodegradability and thermal stability are important starch properties that are commonly focused for modification purposes. Acid hydrolysis has been used for obtaining nanoparticles of various starches (Putaux, Moliuna-Boisseau, Momaur, & Defresne, 2003; Chen et al., 2008; Kim, Lee, Kim, Lim, & Lim, 2012). The idea underlying acid hydrolysis is to exploit the difference in acid susceptibility of amorphous structure and semi-crystalline starch lamellae. Starch hydrolysis with sulphuric and hydrochloric acids produces Nageli amylodextrin and linearized starch, respectively. Acids yield fast hydrolysis of the starch amorphous zones with negligibly slow hydrolysis of crystalline areas. Limited starch acid hydrolysis produces nanocrystals that can be used as fillers in polymeric matrices to improve their mechanical and barrier properties or for stabilizing emulsions (Li, Sun, & Yang, 2012). Starch nanocrystals have been produced from waxy maize starch (Angellier, Choisnard, Molina-Boisseau, Ozil, & Dufresne, 2004; Angellier, Molina-Boisseau, Dole, & Dufresne, 2006; Le Corre, Bras, & Dufresne, 2011; Le Corre, Bras, & Dufresne, 2012; Li et al., 2012).

This work considers the acid hydrolysis of plantain starch. The motivation for using plantain starch for this study relies on the

* Corresponding author.
E-mail addresses: jvc@xanum.uam.mx, jvernoncarter@hotmail.com (E.J. Vernon-Carter).
[1] Tel.: +52 735 3942020; fax: +52 735 3941896.

0144-8617/$ – see front matter © 2013 Elsevier Ltd. All rights reserved.
http://dx.doi.org/10.1016/j.carbpol.2013.03.017

increased interest in using native commodities for developing raw materials for industry, either for producing new products or to replace those products now made from non-renewable sources, for spearheading regional development. Starches from different botanical sources and acid or enzyme hydrolysed modified starches obtained from them are promising candidates for contributing to the achievement of this goal owing to their complete biodegradability, low cost, ready availability and renewability (Lu, Xiao, & Xu, 2009). In this way, the aims of this work were to study: (i) the acid hydrolysis of plantain starch and to determine the kinetics dynamics of the process; (ii) to monitor morphology, crystallinity, structure transition and particle size changes occurring in the hydrolysed granules during hydrolysis time; (iii) to establish an interrelationship between the progression of these parameters with hydrolysis kinetics, in order to gain insights about the underlying phenomena taking place in this complex process, so that eventually a better control may be achieved in the production of plantain starch derivatives with specific functional properties.

2. Materials and methods

2.1. Materials and reagents

Unripe plantain fruits (*Musa paradisiaca* L.) from the variety "Macho" were purchased immediately after harvest (i.e., non-matured with green skin) in the local market in Cuautla, State of Morelos, Mexico. The plantain fruits were not subjected to any postharvest treatment before their use. Sulphuric acid (98%) was obtained from J.T. Baker (Mexico City, Mexico). Food grade sodium sulphate was acquired from BASF Mexicana (Mexico City, Mexico). Deionised water was used in all experiments.

2.2. Starch isolation

Fifty plantain fingers were selected on the basis that they were at least 20 cm long and had green skin colour for the starch isolation, which was done following the procedure reported by Millan-Testa, Mendez-Montealvo, Ottenhof, Farhat, & Bello-Pérez (2005). The plantain fruits (500 g) were peeled, cut into cubes (25–36 cm^3), immediately rinsed in sodium sulphate solution (1.22 g L^{-1}), and then macerated (500 g fruit cubes: 500 g sodium sulphate solution) at low speed in a Waring CAC31 2.0L laboratory blender (LabSource, Manchester, UK) for 2 min. The homogenate was consecutively sieved, washed through screens (50 and 100 US mesh) until the deionised wash water was free from solutes and suspended solids, and centrifuged (Hermle Labortechnik, Z300K, Wehingen, Germany) at 10800 × *g* for 30 min. The white starch sediments were dried in a Precision compact gravity oven (Equipar, S.A. C.V., Mexico City, Mexico) operated at 40 °C for 48 h. The solids were carefully ground with a pestle and mortar to pass through a sieve (US 100 mesh), put into a sealed glass container and stored at room temperature until required.

The chemical composition of the banana starch was determined according to the procedure described by Carmona-García, Sanchez-Rivera, Mendez-Montealvo, Garza-Montoya, & Bello-Pérez (2009), showing the following results: starch expressed as α-glucan of 89.4 ± 2.23%, moisture content of 7.32 ± 0.3%, ash content of 0.29 ± 0.02%, protein content of 1.05 ± 0.05% and fat content of 0.89 ± 0.05% on wet weight. The amylopectin to amylose ratio was 2.44.

2.3. Acid hydrolysis

Acid hydrolysis was carried out according to method reported by Kim et al. (2012) with slight modifications. Starch (15 g, dry basis) was dispersed in an aqueous sulphuric acid solution (100 mL, 3.16 M). Starch and acid solution were maintained dispersed through stirring at 40 °C. Separate suspensions were used for different periods of time (1, 3, 7, 9, 15, 20 days). All experimental runs were implemented in triplicate. For monitoring the hydrolysis advance, the solution was cooled down to 5 °C for recovering non-hydrolysed material, including dissolved and suspended starch granules. Afterwards, the suspension was centrifuged (6000 *g* for 15 min) and the precipitates were washed in distilled water until neutral pH was reached. The precipitated solids were air-dried at 35 °C for 24 h, put into a sealed glass container and stored at 4 °C. In this way, the degree of hydrolysis (%) was calculated as the percent of both suspended solids and dissolved non-hydrolysed starch relative to the initial starch solids.

2.4. Scanning electron microscopy (SEM)

Native and acid hydrolysed plantain starch particles subjected to different hydrolysis times were mounted on carbon sample holders using double-side sticky tape and were observed using a JEOL JMS 7600F scanning electron microscope (Akishima, Japan) with the GB-H mode at 1 kV accelerating voltage. Micrographs at 2000× magnification are presented. Samples were not metalized since the microscopy equipment operates under ultra-vacuum conditions.

2.5. X-ray diffraction (XRD)

Native and acid hydrolysed plantain starch particles subjected to different hydrolysis times were stored for three weeks in a sealed container at a relative humidity of 85% for achieving constant moisture content. XRD patterns were measured at room temperature following a previously reported procedure (Hernández-Nava, Bello-Pérez, San Martín-Martínez, Hernández-Sánchez, & Mora-Escobedo, 2011) with slight modifications. A Siemens D-5000 diffractometer (Karlsruhe, Germany) using Cu Kα radiation (λ = 1.543) and a secondary beam graphite monochromator was operated at 40 kV and 30 mA. Intensities were measured in the 5–70° 2θ range with a 0.03° step size and measuring time of 2.0 s per point.

2.6. Granules particle size distribution and mean size

The particle size distribution of the native and hydrolysed plantain starches was determined with laser diffraction using a Mastersizer 2000 (Malvern Instruments Ltd., Malvern, Worcestershire, UK), with the help of a Scirocco dry disperser unit used for dispersing the powders at a feed pressure of 2 bars and a feed rate of 40%. The obscuration was in the interval of 0.5–5%. The Fraunhofer approximation was used for calculation of the starch granules size distribution and the corresponding volume fraction–length mean diameter ($d_{4,3}$) (Palma-Rodriguez et al., 2012).

2.7. Differential scanning calorimetry (DSC)

Gelatinization properties of native and acid-modified plantain starch particles subjected to different hydrolysis times were analysed by differential scanning calorimetry (DSC) (TA Instruments, Q2000, New Castle, DE, USA) previously calibrated with indium following the procedure described by Palma-Rodriguez et al. (2012) with slight modifications. A starch sample (3.0 mg dry basis) was weighed in an aluminium pan and deionised water (6.0 μL) was added. The mixture was heated in the DSC cell from 20 to 140 °C applying a heating rate of 5 °C min^{-1}. An empty pan was used as the reference.

All measurements were done by triplicate and using the same sample weight. The DSC analysis generates a profile of

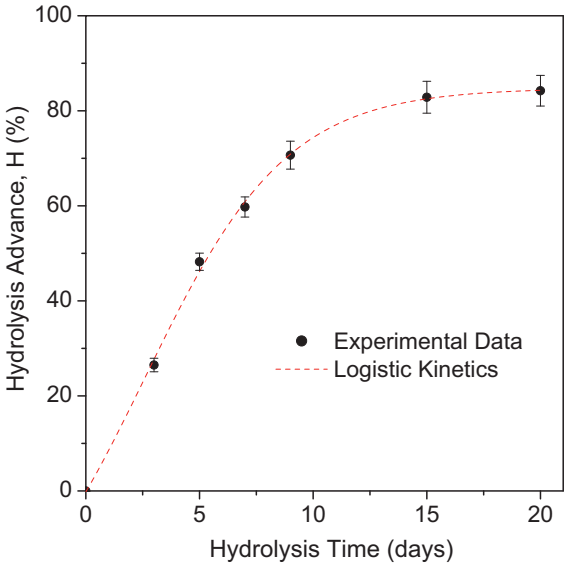

Fig. 1. Experimental data for the hydrolysis advance. The standard deviation was computed from the triplicate measurements for each sampling time. For hydrolysis times non-larger than 15 h, the mean values are significantly different ($p < 0.05$) according to Turkey's test. A logistic kinetics can be used for describing the dynamic behaviour of the hydrolysis advance with time. Note the zero-order kinetics for relatively short (up to about 5–7 days) hydrolysis times.

injected/extracted heat flow from the analysed sample as a function of temperature. Onset, peak and endset temperatures (T_o, T_p and T_e) correspond to the onset, peak and offset of the heat flow with respect to the base line (i.e., sensitive temperature changes). The change in enthalpy corresponds to the integral, within the onset–endset temperature range, of the heat flow profile.

2.8. Statistical analysis

Experimental results are presented as mean ± SEM (standard error of mean) of three different determinations. A commercial package (Sigma Stat 2.03, Jandel Corporation, San Rafael, CA) was used for evaluating significant differences in the means. Statistically significant differences ($p < 0.05$) among means were evaluated using the Turkey multiple comparison procedure.

3. Results and discussion

3.1. Hydrolysis kinetics and percentage

The hydrolysis percentage undergone by the plantain starch during the 20 days period is shown in Fig. 1. The standard deviation was computed from the triplicate measurements for each sampling time. For hydrolysis times non-larger than 15 h, the mean values were significantly different ($p < 0.05$). A two-stage hydrolysis behaviour can be observed, with a fast hydrolysis in the early days (between 0 and 7 days), followed by a slower stage (between 7 and 15 days) until non-hydrolysis stage was attained at about the 20th day. Depending on the botanical source, different levels of structure may govern the hydrolysis pattern and rate of starch granules. The first hydrolysis stage is presumably due to the hydrolysis of the amorphous regions of starch granules (Kainuma & French, 1971; Le Corre et al., 2011; Kim et al., 2012). The second hydrolysis stage reflects a slower hydrolysis that is commonly related to the degradation of semi-crystalline and crystalline regions (Le Corre et al., 2011). This suggests that the dynamics of the hydrolysis advance can be described by a logistic kinetics of the form

$$\frac{dH}{dt} = \mu_{\max}\left(\frac{1-H}{H_{\max}}\right), \quad \text{for} \quad 0 \le H \le H_{\max},$$

where H is the hydrolysis advance, $H_{\max}$ is the maximum achievable acid hydrolysis and $\mu_{\max}$ is the maximum hydrolysis rate. Fig. 1 also shows the fitting of this kinetics expression by means of numerical least-square methods. The estimated maximum hydrolysis rate and maximum achievable hydrolysis extent were $\mu_{\max} = 9.22 \pm 0.46\%$/day and $H_{\max} = 84.76 \pm 1.39\%$, respectively. The extent of the hydrolysis achieved at day 20 was ca. of 82%.

3.2. SEM study

The native and acid treated starches obtained at different hydrolysis times were observed by SEM (Fig. 2). Native starch granules exhibited a regular, oval-like shape with smooth surface. After the third day of hydrolysis, only some starch granule presented slight erosion and fractures on the surface, gradually increasing by the fifth day, but with most of the starch granules maintaining their oval shapes. At longer hydrolysis times (5 days and thereafter), several phenomena were observable. Firstly, deformations on the surface of acid-treated granules occurred. There is evidence of adhesion between some of the granules (days 5, 7 and 9), with progressively more profound surface erosion that eventually led to the fragmentation of some of the starch granules. This pattern became more prominent at the final stage of the hydrolysis time (20 days). The presence of some residual small granules after the 15 days was observed. Kim et al. (2012) showed that nanocrystals can be obtained after 5–7 days of acid hydrolysis when the amorphous lamellae of starches were eroded and nano crystalline components could be released from growth rings. In principle, the number of starch nanocrystals should increase at longer acid hydrolysis time. In this work hydrolysed starch granules with irregular shape produced by the agglomeration of fragments were observed. Furthermore, some fragmented granules generated by fracture of highly eroded granules were also evident. This heterogeneity in the shape and size of the hydrolysed granules arose because not all of the native starch granules had the same size and shape. Additionally, the stirring during the acid hydrolysis process could have favoured the fragmentation of the starch granules (Le Corre et al., 2011). These results corroborate previous findings indicating that the arrangement of starch components in the concentric rings have important effects in the rate of acid hydrolysis for producing starch nanocrystals. Le Corre et al. (2011) and Kim et al. (2012) reported different findings for the acid hydrolysis with sulphuric acid (~3–3.16 M) of waxy maize starch. The former researchers found that after 5 days of treatment the starch granules were fully hydrolysed while the latter investigators showed that crystalline structures still prevailed after 5 days. More studies are necessary along this research line to clarify the discrepancies between works.

3.3. XRD study

XRD patterns of native plantain starch and the hydrolysed fractions at different times are shown in Fig. 3. The dotted vertical lines are used for highlighting three prominent intensity peaks at about 15.0, 17.5 and 23.0 diffraction degrees, which are indicative of A-type crystallinity. Our results agree with those of Millan-Testa et al. (2005), reporting the same three prominent peaks described in Fig. 3. Additionally, a small peak at 5.4 diffraction degrees indicative of the presence of B-type crystals was also displayed for native and relatively small hydrolysis times. Starches containing both A- and B- polymorph forms are called C-type starches (Wang, Bogracheva,

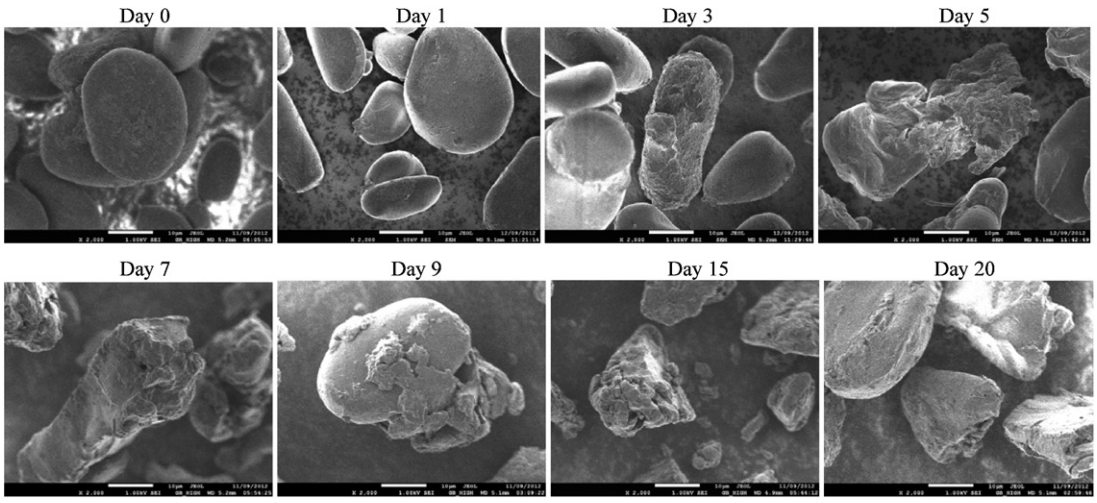

Fig. 2. SEM images (2000×) for different hydrolysis times. For short times, the starch granules maintain the oval shape, but at longer times the acid hydrolysis erodes the granule surface, yielding fractured granules.

& Hedley, 1998; Tester, Karkalas, & Qi, 2004; Gernat, Radosta, Damaschun, & Schierbaum, 2006). The peak at 17.5° was much more prominent than that at 15.0°, and the peak at 23° was broader. These intensity peaks appeared in the native and in all of the hydrolysed fractions. In the first hydrolysis stage, the intensity of the peaks gradually increased from day 1 to day 7. This indicates that the relative fraction of the crystalline regions increased due to the hydrolysis of the amorphous regions of the starch granules. However, a decrease in the peaks intensity occurred from day 7 to day 9. By day 15 very small peaks were observed, and by day 20 the peaks were merely discernible, accounting for ~18% of non-hydrolysed remaining residue.

Given the small intensity peak at 5.4° in the XRD analysis (Fig. 3), the plantain crystallinity is dominated by A-type structures. Evidence that the B-type crystalline structure is a relatively minor component of plantain starch is provided by the disappearance in the first days of the hydrolysis process of the 5.4° XRD intensity peak (Fig. 3). Robin, Mercier, Charbonnière, & Guilbot (1974)

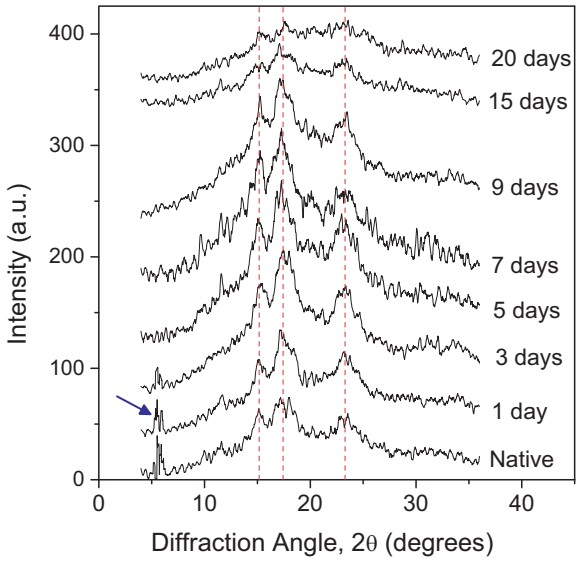

Fig. 3. XRD patterns for the different hydrolysis times. The dotted vertical lines are used for highlighting three prominent intensity peaks at about 15.0°, 17.5° and 23.0°, characteristic of A-type crystallinity, while the arrow pinpoints a small peak at 5.4° indicative of the presence of B-type crystals. The relative value of the intensity peaks is changed as the hydrolysis advances in time.

reported that as a rule of thumb starches with A-type XRD pattern (e.g. waxy and normal maize) are more susceptible to acid hydrolysis than B-type starches (e.g. potato and high amylose maize). However, Kim et al. (2012) reported that A-type starches are more resistant to acid hydrolysis than B-type starches. A-type crystalline structures exhibit densely packed unit cells, which presumably are more resistant to hydrolysis. It is apparent that the susceptibility of starches to hydrolysis may be affected by other factors as well, such as the branching location of internal chains, i.e. the clustered versus scattered branching structure. The amorphous regions of plantain starch are certainly more resistant to acid hydrolysis than those of waxy and normal maize, perhaps because the amylose chains are inter-dispersed in the amorphous regions of amylopectin (branch points). The higher amylose content (37%) of plantain starch (Aparicio-Saguilán et al., 2005) and the dense package of the double helices of the lineal chains of amylopectin in the crystalline regions (Li et al., 2012; Le Corre et al., 2011) contribute for the relative slow hydrolysis rate of the plantain starch as compared to other starch sources (e.g., waxy and normal maize).

Two crystallinity indices were used for quantifying crystallinity changes as function of the hydrolysis time. The first one considers that the most prominent intensity peak is located at 17.5° diffraction angle. In this way, a crystallinity index relative to the native starch is defined as

$$CI_{17.5} = \frac{I_{17.5}}{I^N_{17.5}} \times 100$$

where $I_{17.5}$ and $I^N_{17.5}$ are respectively the intensity for sample and native starches at 17.5°. The second crystallinity index accounts for the average change of the intensity pattern of the main intensity peaks by introducing the following relationship:

$$\langle CI \rangle = \frac{\int_{2\theta_{min}}^{2\theta_{max}} I(2\theta)d(2\theta)}{\int_{2\theta_{min}}^{2\theta_{max}} I^N(2\theta)d(2\theta)} \times 100$$

for the diffraction range $2\theta_{min} = 5$ and $2\theta_{max} = 35°$. It should be pointed out that the computation of the integrals is performed after removing the baseline for all XRD patterns. In this way, the ratio for the average crystallinity index is computed under the

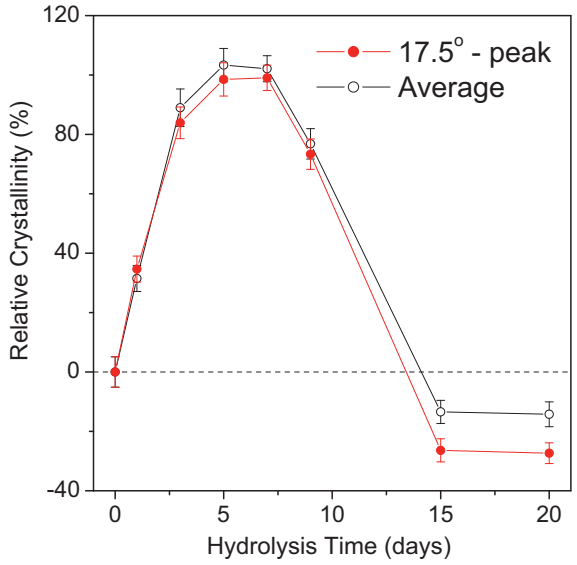

Fig. 4. Relative crystallinity indices as function of the hydrolysis time. A maximum is achieved at about 5–7 days, coinciding with the end of the zero-order hydrolysis kinetics.

same detrended baseline. Fig. 4 presents the relative crystallinity indices as a function of the hydrolysis time. Note that both indices exhibit similar quantitative behaviour, indicating that changes in crystallinity are not constrained to specific structures (like that represented by the 17.5° peak), but to the whole crystalline configuration. As already observed above, the crystallinity indices achieved a maximum value (about a 100% increment) in between 5 and 7 days hydrolysis time. Afterwards, the crystallinity decreased to achieve values similar to that for native starches. This corroborates previous findings establishing that, in a first stage, acidic hydrolysis affects predominantly the amorphous regions, so that residual starch has a more refined crystallinity. The results in Fig. 4 suggest that the crystallinity indices introduced above can be used as suitable quantities for monitoring the evolution of starch crystallinity during acidic hydrolysis in order for obtaining, e.g., starch granules with maximum crystallinity content. It is noted that the maximum crystallinity increase coincides with the end of the first hydrolysis stage corresponding to zero order kinetics. Finally, the decreased crystallinity for long hydrolysis times suggests that the acid degraded mainly amylose and long amylopectin chains, leading to an increment in the proportion of amorphous short chains.

3.4. Particle size distribution (PSD)

PSD was used for further evaluating the effects of hydrolysis on starch granules. Fig. 5a presents the PSD for native plantain starch and for the hydrolysates obtained at 5, 9 and 20 days. The evolution of $d_{4,3}$ is exhibited in Fig. 5b. Native starch showed a log-normal PSD, which is typical of particulate systems. Under the acid action, the span of the distribution broadens with the peak shifting increasingly to the right as hydrolysis time proceeds, resulting in an increase in the mean particle diameter. Such diameter increase can be caused by two factors, namely: (i) the erosion of the amorphous regions during the first 5–7 days, which can promote water migration into the inter-lamellae regions. In fact, it has been suggested (Donovan, 1979) that in excess water (i.e., the hydrolysis conditions), amorphous lamellae absorb water and expand. In turn, this process can lead to partial gelatinization (and swelling) in located regions of the starch granules; and (ii) released hydrolysates can undergo retrogradation, yielding small-size particles that adhere unto larger starch granules. The resulting granules have a quite

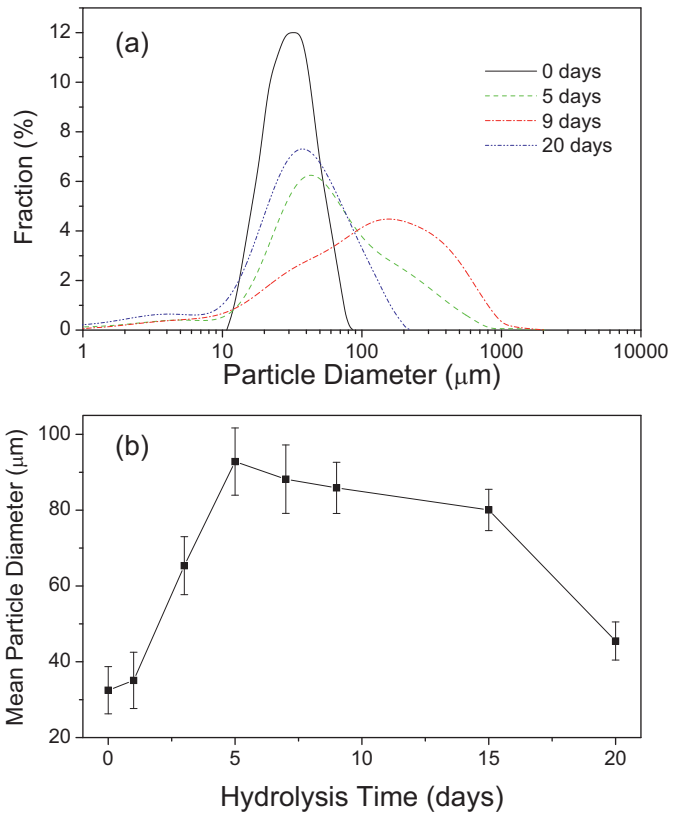

Fig. 5. (a) PSD for four different hydrolysis times. It is noted that the PSD moves rightward, indicating an increase of the mean particle diameter. (b) Mean particle diameter as function of the hydrolysis time. Similar to the crystallinity index in Fig. 4, the mean particle diameter achieves a maximum after about 5–7 days of hydrolysis time.

irregular shape (see Fig. 2) where the original oval geometry is not longer found. For longer hydrolysis times (more than 5–7 days), the mean particle declines to attain values similar to that of the native starch, although with granules with fractures and irregular shape (see Fig. 2). Interestingly, similar to the crystallinity behaviour shown in Fig. 4, the maximum mean particle diameter coincides with the end of the first hydrolysis stage (see Fig. 1) when the hydrolysis rate follows zero order kinetics. This can be seen as a further support for a two-stage hydrolysis model where the granule structure is changed differently at relatively small and long hydrolysis times.

3.5. DSC analysis

The onset, peak and endset temperatures (T_o, T_p and T_e) and enthalpy change (ΔH) shown by the plantain native and acid hydrolysed starches subjected to a heating ramp are shown in Table 1. The samples hydrolysed for 1 and 3 days presented a slight decrease in T_o but T_p and T_e increased. These results are in line with the SEM study that in the early days of the acid hydrolysis, regular granular structures were observed, with only slight changes in the surface morphology of the starch granules. Such behaviour is in agreement with that determined in normal and waxy maize starches hydrolysed for 5 days (Kim et al., 2012). At longer hydrolysis times (between 5 and 15 days) an increase in To occurred, and these values are similar to that of plantain native starch. Regarding T_p and T_e, the values increased with the hydrolysis time, maybe caused by annealing effects during the hydrolysis process. In contrast, the enthalpy displayed only relatively small increments in line with the changes in the crystallinity index in Fig. 4. The range of the

Table 1
DSC analysis parameters of native and acid-hydrolysed starch.

	Hydrolysis time (days)	T_o (°C)	T_p (°C)	T_e (°C)	ΔH (J/g)	T_e–T_o (°C)
Native starch	–	74.6 ± 0.5^{ad}	87.6 ± 0.6^{a}	101.6 ± 0.9^{a}	15.1 ± 0.4^{a}	27.3 ± 0.5^{a}
Hydrolysed starch	1	71.2 ± 0.3^{b}	88.1 ± 0.2^{b}	103.5 ± 1.1^{b}	16.9 ± 0.2^{a}	32.7 ± 0.8^{bc}
	3	70.8 ± 0.5^{c}	88.8 ± 0.3^{c}	104.6 ± 0.8^{b}	19.8 ± 0.1^{a}	32.0 ± 0.6^{b}
	5	70.4 ± 0.1^{c}	90.7 ± 0.3^{d}	104.8 ± 0.5^{c}	22.7 ± 0.3^{bc}	31.9 ± 0.3^{b}
	7	74.6 ± 0.5^{a}	93.6 ± 0.3^{e}	106.9 ± 0.7^{c}	24.6 ± 0.2^{a}	32.1 ± 0.2^{b}
	9	75.1 ± 0.4^{d}	95.4 ± 0.7^{f}	109.5 ± 0.6^{d}	21.4 ± 0.2^{b}	33.5 ± 0.7^{c}
	15	75.8 ± 0.6^{d}	97.4 ± 0.4^{g}	111.1 ± 0.9^{e}	21.8 ± 0.3^{c}	36.5 ± 0.1^{d}
	20	–	–	–	–	–

Values are means ± SD of three replicates. Significant differences in each column are expressed as different letter ($p < 0.05$). T_o, T_p and T_e correspond to onset, peak and endset temperatures; ΔH is the enthalpy change, T_e–T_o is the gelatinisation temperature range.

(Te–To) increased as the acid treatment time increased, indicating that the crystallinity heterogeneity was broader for the hydrolysed granules. The increase in T_p and T_e with the acid hydrolysis was related with the removal of the amorphous regions of starch granules, due to the melting of the remaining crystalline regions at higher temperature, but without altering the content and perfection of the double helices of amylopectin, which was reflected by relatively small increments of the enthalpy values (Le Corre et al., 2011). It should be commented that Kim et al. (2012) reported that high amylose maize starch, potato starch and mungbean starch did not show structure transition after 5 days of acid hydrolysis, as reflected in XRD patterns. However, the former technique assessed the short-range order and XRD the long-range order, and consequently DSC results should be obtained if XRD diffraction peaks are present. At the longest hydrolysis time (20 days), no crystalline structure transition was observed. As already indicated by previous studies of starch hydrolysis (Le Corre et al., 2011), this can be seen as an indicative that the plantain starch nanocrystals were fully hydrolysed, a result that that is in agreement with the X-ray diffraction pattern where the detected intensity peaks were not well-defined.

It should be pointed out that calorimetric determinations are not sufficient for a tight monitoring of the starch hydrolysis process. These measurements should be complemented by additional analysis, such as XRD analysis. For instance, the peak temperature (Table 1), although monotonously increasing with respect to the hydrolysis time, indicated continuous structural changes although the acid hydrolysis showed no further advance. For industrial applications, DSC is a non-expensive technique for monitoring the first hydrolysis stage. However, XRD should aid the process off-line monitoring for relatively long hydrolysis times.

4. Conclusions

This work used different analysis techniques for monitoring the dynamics of starch acid hydrolysis. The study considered plantain native starch, a C-type crystalline structure, as a case study. The results derived from microscopy, X-ray diffraction patterns, particle size distribution and differential scanning calorimetry analyses showed consistent results in the sense that the amorphous fractions were firstly hydrolysed following zero-order kinetics. An apparent structure transition was detected for intermediate hydrolysis times, which might be related to a rearrangement of short crystalline chains that are harder to hydrolyse than amorphous fractions. Such transition was accompanied by a decrement of crystallinity and mean particle diameter, as well as by a sharp reduction of the endothermic heat flow. Overall, the results in this work showed that acid hydrolysis is a complex process underlying starch microstructure changes with crystalline transition, which can be detected by available analysis techniques.

Acknowledgements

The authors wish to acknowledge the partial financial support of this research to the Instituto de Ciencia y Tecnología del Distrito Federal (ICyTDF) through project PICSO11-64, and also to SIP-IPN, COFAA-IPN and EDI-IPN. Author LABP wishes to thank the Universidad Autónoma Metropolitana-Iztapalapa for visiting professorship grant.

References

Angellier, H., Choisnard, L., Molina-Boisseau, S., Ozil, P., & Dufresne, A. (2004). Optimization of the preparation of aqueous suspensions of waxy maize starch nanocrystals using a response surface methodology. *Biomacromolecules*, *5*, 1545–1551.

Angellier, H., Molina-Boisseau, S., Dole, P., & Dufresne, A. (2006). Thermoplastic starch-waxy maize starch nanocrystals nanocomposites. *Biomacromolecules*, *7*, 531–539.

Aparicio-Saguilán, A., Flores-Huicochea, E., Tovar, J., García-Suárez, F., Gutiérrez-Meraz, F., & Bello-Pérez, L. A. (2005). Resistant starch-rich powders prepared by autoclaving of native and linearized banana starch: partial characterization. *Starch/Stärke*, *57*, 405–412.

Bello-Pérez, L. A., & Paredes-López, O. (2009). Starches of some crops, changes during processing and their nutraceutical potential. *Food Engineering Reviews*, *1*, 50–65.

Biliaderis, C. G. (1991). The structure and interactions of starch with food constituents. *Canadian Journal of Physiology and Pharmacology*, *69*, 60–78.

Carmona-García, R., Sanchez-Rivera, M. M., Mendez-Montealvo, G., Garza-Montoya, B., & Bello-Pérez, L. A. (2009). Effect of the cross-linked reagent type on some morphological, physicochemical and functional characteristics of banana starch (*Musa paradisiaca*). *Carbohydrate Polymers*, *79*, 117–122.

Chen, G., Wei, M., Chen, J., Huang, J., Dufresne, A., & Chang, P. R. (2008). Simultaneous reinforcing and toughening: new nanocomposites of waterborne polyurethane filled with low loading level of starch nanocrystals. *Polymer*, *49*, 1860–1870.

Donovan, J. W. (1979). Phase transitions of the starch–water system. *Biopolymers*, *18*, 263–275.

Gallant, D. J., Bouchet, B., & Baldwin, P. M. (1997). Microscopy of starch: evidence of a new level of granule organization. *Carbohydrate Polymers*, *32*, 177–191.

Gernat, S., Radosta, G., Damaschun, G., & Schierbaum, F. (2006). Supramolecular structure of legume starches revealed by X-ray scattering. *Starch/Stärk*, *42*, 175–178.

Hernández-Nava, R. G., Bello-Pérez, L. A., San Martín-Martínez, E., Hernández-Sánchez, H., & Mora-Escobedo, R. (2011). Effect of extrusion cooking on the functional properties and starch components of lentil/banana blends: response surface analysis. *Revista Mexicana de Ingeniería Química*, *10*, 409–419.

Kainuma, K., & French, D. (1971). Naegelli amylodextrin and its relationship to starch granule structure I. Preparation and properties of amylodextrins from various starch types. *Biopolymers*, *10*, 1673–1680.

Kim, H. Y., Lee, J. H., Kim, J. Y., Lim, W. J., & Lim, S. T. (2012). Characterization of nanoparticles prepared by acid hydrolysis of various starches. *Starch/Stärke*, *64*, 367–373.

Le Corre, D., Bras, J., & Dufresne, A. (2011). Evidence of micro- and nanoscaled particles during starch nanocrystals preparation and their isolation. *Biomacromolecules*, *12*, 3039–3046.

Le Corre, D., Bras, J., & Dufresne, A. (2012). Influence of native starch's properties on starch nanocrystals thermal properties. *Carbohydrate Polymers*, *87*, 658–666.

Li, Ch., Sun, P., & Yang, Ch. (2012). Emulsion stabilized by starch nanocrystals. *Starch/Stärke*, *64*, 497–502.

Lu, D. R., Xiao, C. M., & Xu, S. J. (2009). Starch-based completely biodegradable polymer materials. *Express Polymer Letters*, *3*, 366–375.

Millan-Testa, C. E., Mendez-Montealvo, M. G., Ottenhof, M. A., Farhat, I. A., & Bello-Pérez, L. A. (2005). Determination of the molecular and structural characteristics of okenia, mango, and banana starches. *Journal of Agricultural and Food Chemistry*, *53*, 495–501.

Oates, C. G. (1997). Towards an understanding of starch granule structure and hydrolysis. *Trends in Food Science and Technology*, *8*, 375–382.
Palma-Rodriguez, H. M., Agama-Acevedo, E., Mendez-Montealvo, G., Gonzalez-Soto, R. A., Vernon-Carter, E. J., & Bello-Pérez, L. A. (2012). Effect of acid treatment on the physicochemical and structural characteristics of starches from different botanical sources. *Starch/Stärke*, *64*, 115–125.
Putaux, J. L., Moliuna-Boisseau, S., Momaur, T., & Defresne, A. (2003). Platelet nanocrystals resulting from the disruption of waxy maize starch granules by acid hydrolysis. *Biomacromolecules*, *4*, 1198–1202.
Robin, J. P., Mercier, C., Charbonnière, R., & Guilbot, A. (1974). Lintnerized starches gel filtration and enzymatic studies of insoluble residues from prolonged acid treatment of potato starch. *Cereal Chemistry*, *51*, 389–406.
Tester, R. F., Karkalas, J., & Qi, X. (2004). Starch-composition, fine structure and architecture. *Journal of Cereal Science*, *39*, 151–165.
Wang, T. L., Bogracheva, T. A., & Hedley, C. L. (1998). Starch: as simple as A, B, C? *Journal of Experimental Botany*, *49*, 481–502.